Microfluid Nanofluid (2011) 11:209–220
DOI 10.1007/s10404-011-0788-3

RESEARCH PAPER

A disposable, integrated loop-mediated isothermal amplification cassette with thermally actuated valves

Changchun Liu · Michael G. Mauk · Haim H. Bau

Received: 16 January 2011 / Accepted: 10 March 2011 / Published online: 18 March 2011

Abstract An inexpensive, disposable, integrated, polymer-based cassette for loop-mediated isothermal amplification (LAMP) of target nucleic acids was designed, fabricated, and tested. The LAMP chamber was equipped with single-use, thermally actuated valves made with a composite consisting of a mixture of PDMS and expandable microspheres. The effect of the composite composition on its expansion was investigated, and the valve's performance was evaluated. In its closed state, the valve can hold pressures as high as 200 kPa without any significant leakage. Both the LAMP chamber and the valves were actuated with thin film heaters. The utility of the cassette was demonstrated by carrying out LAMP of *Escherichia coli* DNA target and reverse transcribed loop meditated isothermal amplification (RT-LAMP) of RNA targets. The amplicons were detected in real time with a portable, compact detector. The system was capable of detecting as few as 10 target molecules per sample in well under 1 h. The portable, integrated cassette system described here is particularly suited for applications at the point of care and in resource-poor countries, where funds and trained personnel are in short supply.

Keywords Integrated microfluidic cassette · Loop-mediated isothermal amplification (LAMP) · Thermally actuated PDMS valves · *Escherichia coli* · Nucleic acid detection · Real-time fluorescence quantification · Expandable microsphere · Thermal actuation

Electronic supplementary material The online version of this article (doi:10.1007/s10404-011-0788-3) contains supplementary material, which is available to authorized users.

C. Liu · M. G. Mauk · H. H. Bau (✉)
Department of Mechanical Engineering and Applied Mechanics, University of Pennsylvania, 229 Towne Building, 220 S. 33rd St., Philadelphia, PA 19104-6315, USA
e-mail: bau@seas.upenn.edu

1 Introduction

Nucleic acid amplification is an indispensable step in molecular diagnostics. Recently, there has been an increasing interest in point of care and home genetic diagnostic platforms using microfluidic chip technology (Yager et al. 2006; Easley et al. 2006; Chen et al. 2007; Liu et al. 2009). A great amount of effort has been invested in developing microfluidic chips for polymerase chain reaction (PCR) (Chen et al. 2004; Auroux et al. 2004; Zhang et al. 2006; Zhang and Xing 2007; Wang et al. 2006; House et al. 2010). Although PCR is a well established and widely used technology for DNA amplification, the need for thermal cycling complicates the use of PCR at point of care settings and increases the cost of PCR-based devices.

As an alternative to PCR, various isothermal nucleic-acid amplification methods have been proposed (Compton 1991; Walker et al. 1992; Piepenburg et al. 2006; Notomi et al. 2000). Isothermal nucleic-acid amplification technologies are more suitable for point of care diagnostics as they require less complex thermal control than PCR. Lutz et al. (2010) demonstrated a recombinase polymerase amplification (RPA)-based lab-on-a-foil for the detection of the antibiotic resistance gene *mecA* of *Staphylococcus aureus*. Gulliksen et al. (2005) and Dimov et al. (2008) reported, respectively, on using nucleic acid sequence-based amplification (NASBA) microfluidic chips for the detection of the human papilloma virus (HPV) and *Escherichia coli* bacteria. Sato et al. (2010) demonstrated a microbead-based, rolling circle amplification (RCA)

microchip for *Salmonella* detection. Fang et al. (2010) developed a microchip-based, loop-mediated isothermal amplification (LAMP) system for pseudorabies virus (PRV) detection. Ramalingam et al. (2009) reported combining helicase dependent amplification (HDA) with microchip technology for amplifying the BNI-1 fragment of SARS cDNA.

The devices reported above focus on the reaction chamber and do not integrate valves into the device. It is desirable to seal the reaction chamber to reduce the introduction of contaminants and to prevent evaporation as the nucleic acid amplification process takes place at an elevated temperature. Although valveless technologies have been developed to reduce evaporation (Zhang and Xing 2010), valves are still predominantly used for sealing in microfluidics (Chen et al. 2007; Wang et al. 2006; Das et al. 2007; Oh and Ahn 2006). Diverse, ingenious actuation mechanisms for microfluidic valves have been developed such as piezoelectric (Li et al. 2004; Shao et al. 2004), magnetic (Bae et al. 2002; Gaspar et al. 2008), thermal (Kim et al. 2004; Chen et al. 2008), pneumatic (Lagally et al. 2004; Lien et al. 2009), and hydraulic (Oh et al. 2005). Thermal actuation, which does not require moving components, is often adopted in microfluidic chips because of its simplicity, low cost, and reliability (Liu et al. 2004, 2002; Chen et al. 2005; Wang et al. 2005). However, thermally actuated valves, such as ice valves, require a continuous power supply during their entire actuation time, which is undesirable for a reactor operating for as long as an hour. Moreover, in many nucleic acid amplification reactors with real-time detection, in which the amplification products need not be further processed after detection, a single action "one-shot" valve would suffice. Recently, Stemme's group reported on a simple, easy to fabricate, thermally responsive, single action valve cast with a mixture of PDMS and expandable Expancel® microspheres (Samel et al. 2007a, b).

In this paper, we report on a plastic, disposable cassette consisting of a reaction chamber for isothermal amplification of nucleic acids and two thermally actuated valves made with a PDMS–expandable microsphere composite. Prior to the amplification process, the valves were heated, expanded, and sealed the amplification reactor. The amplification process was monitored in real time with a minute detector. The paper describes the design and construction of the cassette and characterizes, for the first time, the expandability of the PDMS–expandable microsphere composite as a function of the PDMS' composition and dopant concentration. The dopants were added to augment the thermal conductivity of the PDMS. Furthermore, we demonstrated the utility of the integrated device by amplifying, with LAMP, both DNA and RNA targets. As an example of a DNA target, we used the *E. coli* pathogen, which causes infections of extraintestinal sites such as the urinary tract and meninges. As an example of a RNA target, we used the RNA control included in the reverse transcription, loop-mediated, isothermal amplification (RT-LAMP) kit provided by the Eiken Chemical Co. In a separate work, we used the LAMP process to amplify and detect HIV RNA (Liu et al. 2011).

2 LAMP cassette and reagents

2.1 LAMP cassette

The 46 mm × 36 mm × 3.37 mm cassette consists of three layers of polycarbonate (McMaster Carr, Atlanta, GA, USA) (Fig. 1a): a top, 120 μm thick, polycarbonate film; a 3.0 mm thick cassette body; and a bottom, 250 μm thick polycarbonate film. The various layers were solvent-bonded with acetonitrile at room temperature. Figure 1a

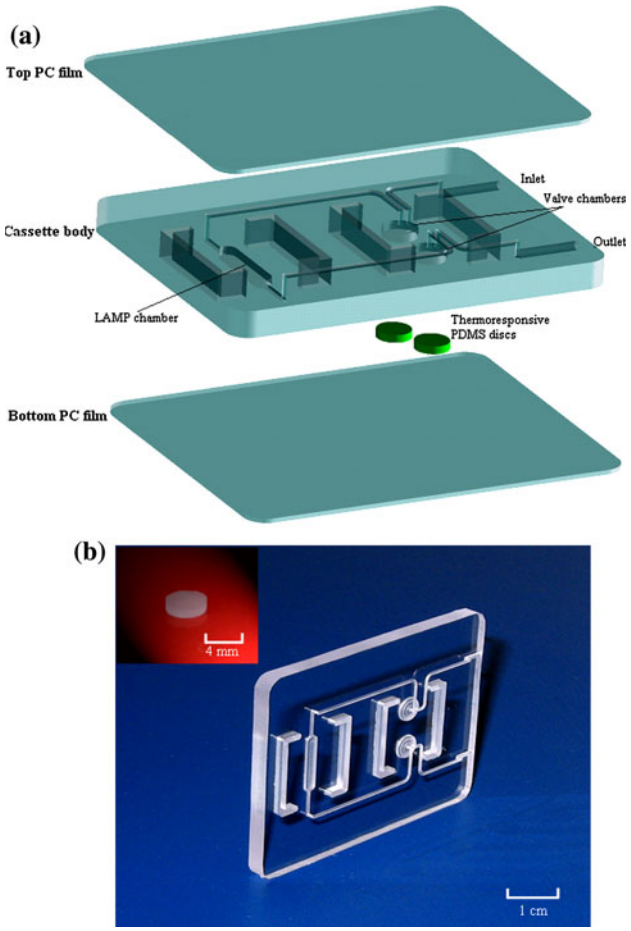

Fig. 1 The LAMP cassette: **a** exploded view of the cassette. The cassette consists of three solvent-bonded layers of polycarbonate. The various features are milled in the main body of the cassette. Also shown are the thermoresponsive, PDMS disks that form the valves. **b** A photograph of the LAMP cassette body. The *inset* is a photograph of the thermoresponsive PDMS disk

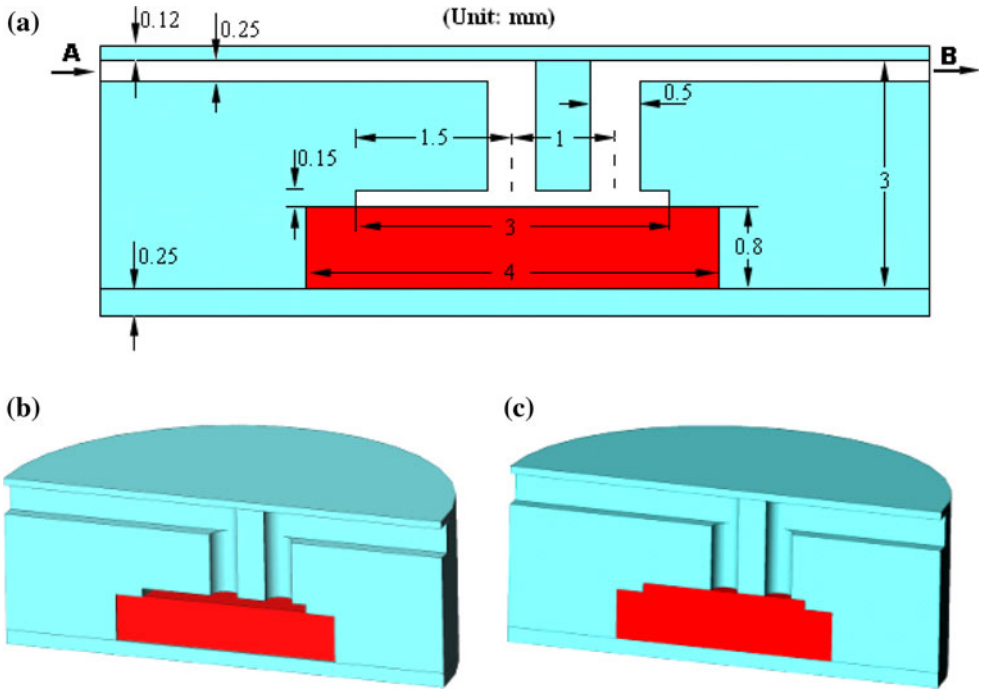

Fig. 2 Thermo-responsive PDMS-based, single action, normally open valve. **a** Valve cross-section (*open state*) and valve's dimensions. **b** Three-dimensional rendering of the valve in open state. **c** Three-dimensional rendering of the valve in closed state

and b are, respectively, an exploded view of the cassette and a photograph of the cassette's body. The cassette's body was fabricated using a precision, computer-controlled (CNC) milling machine (HAAS Automation Inc., Oxnard, CA) (Liu et al. 2009). The cassette has two functional domains: a LAMP/RT-LAMP incubation (reaction) chamber and two valve chambers. The reaction chamber is connected to the valve chambers with 500 μm wide and 250 μm deep conduits with rectangular cross-sections. Inlet and exit ports, each 0.8 mm in diameter, were drilled (with a tabletop milling machine, MF 70, Proxxon, Niersbach, Germany) in the side of the main body of the cassette (Fig. 1a). One valve chamber is connected to the inlet port, and the other valve chamber is connected to the exit port.

The reaction chamber is 10 mm in length, 2.0 mm in width, 1.0 mm in depth, and 20 μL in volume. The chamber is located at the bottom of the cassette's main body, and it is separated from the heater by the 250 μm thick, bottom polycarbonate film. The inlet and outlet conduits of the reaction chamber are connected through vertical vias to conduits milled in the upper surface of the main body. To improve thermal isolation, the reaction chamber is surrounded by air-filled cavities.

Each valve chamber consists of a 4 mm diameter, 0.8 mm deep well to house a thermo-responsive, PDMS composite disk and a shallow 3 mm diameter, 150 μm deep compartment to facilitate fluid flow when the valve is open (Fig. 2). Figure 2a depicts the cross-section of the assembled valve (all the dimensions are given in mm). The valve structure will be described in detail in Sect. 2.2. The valves' compartments were milled in the bottom surface of the main cassette body. Like the reaction chamber, the valves are surrounded by air-containing cavities to provide thermal isolation.

2.2 Thermo-responsive PDMS valves

The valve was formed with a composite of PDMS (Sylgard 184 Silicone Elastomer Kit, Dow Corning) and highly expandable microspheres (Expancel 031 DUX 40, Duluth, GA). Expancel microspheres consist of ~10 μm diameter spherical shells, made with vinylidene chloride, acrylonitrile, and methyl methacrylate, and filled with pressurized liquid hydrocarbon such as isobutane and isopentane. When the microsphere is heated above 80°C, the hydrocarbon undergoes a phase transition into a gas and inflates the shell. Due to the elevated temperature, the shell material is soft and undergoes plastic deformation. As a result, the sphere's diameter increases approximately four-fold and its volume increases by a factor of ~60. This transition is essentially irreversible. Once the sphere is cooled, it remains in its expanded state (Roxhed et al. 2006; Griss et al. 2002).

To prepare the PDMS–expandable microsphere composite, we mixed the PDMS base, a curing agent, and expandable microspheres at predetermined ratios, and degassed the mixture in vacuum. In some of our experiments, we added silver powder (2–3.5 μm diameter particles with 99.9% purity, Sigma-Aldrich, St. Louis, MO) to the mixture to enhance the thermal conductivity of the composite. Various blend compositions were tested (Sect. 4.2). The suspension was carefully cast in a

polycarbonate mold consisting of 0.8 mm deep, 4 mm diameter milled wells (Fig. S1). Subsequently a flat, 5 mm thick polycarbonate slab was slowly placed over the PDMS–expandable microspheres suspension, allowing surface tension to pull the polycarbonate slab into intimate contact with the prepolymer without any bubble formation at the interface. To prevent the suspended microspheres from prematurely expanding, the curing of the PDMS–expandable microspheres composite was carried out at 60°C (i.e., below the phase transition temperature of the microspheres) for about 4 h.

Figure 2 depicts the normally open valve. Figure 2a is a cross-section of the valve in its open state. Figure 2b and c are, respectively, three-dimensional renderings of the open valve and closed valve. When the valve is in an open state (Fig. 2a, b), fluid is free to flow from conduit A to conduit B. When the valve is heated, the PDMS composite expands and permanently seals the passage between conduits A and B.

2.3 Reagents and protocol for DNA LAMP

On-chip LAMP was carried out in the 20 μL LAMP reaction chamber at 63°C. For a description of the LAMP process, see Notomi et al. (2000) and Nagamine et al. (2002). The LAMP template (plasmid DNA), extracted from pathogenic *E. coli* was obtained from urine samples, and the primers for *E. coli* were a gift from Professor Abhay Vats (Department of Pediatrics, Children's Hospital of Pittsburgh, Pittsburgh, Pennsylvania, USA). The primers and their respective concentrations for *E. coli* DNA amplification were: outer primer F3 5′-GCCATCTCCTGA TGACGC-3′ (0.2 μM), outer primer B3 5′-ATTTA CCGCAGCCAGACG-3′ (0.2 μM), loop primer F loop 5′-CTTTGTAACAACCTGTCATCGACA-3′ (0.8 μM), loop primer B loop 5′-ATCAATCTCGATATCCATGAAGG TG-3′ (0.8 μM), inner primer BIP 5′-CTGGGGCGAGG TCGTGGTATTCCGACAAACACCACGAATT-3′ (1.6 μM) and inner primer FIP 5′-CATTTTGCAGCTGTA CGCTCGCAGCCCATCATGAATGTTGCT-3′ (1.6 μM) (Hill et al. 2008). The reaction mixture also contained 20 mM Tris–HCl (pH 8.8) (Fisher Scientific, Inc., PA), 10 mM KCl, 10 mM $(NH_2)_2SO_4$, 2 mM $MgSO_4$, 0.1% Triton X-100 (Sigma Chemical Co., MO), 0.8 M betaine (Sigma-Aldrich, St. Louis, MO), 8 U of Bst DNA polymerase (New England Biolabs, Inc., MA), 1.4 mM dNTPs (Promega, WI), 4.0 μM SYTO® 9 Green (Molecular Probes, Inc., Eugene, OR), and 5 μL of *E. coli* DNA at various concentrations. DNase/RNase-free water (Fisher Scientific, Inc., PA) was used throughout the experiments.

To confirm the real-time fluorescence detection, at the end of the experiment, we drilled into the reactor and removed the reaction products with a pipette. The LAMP reaction products were analyzed by gel electrophoresis. 3 μL of each LAMP-amplified product was loaded onto a lane of a 2.0% agarose gel. Electrophoresis of the amplified DNA fragment was carried out in Tris–Acetate–EDTA (TAE) buffer at a constant voltage of 114 V for 40 min. DNA marker VIII (Roche Diagnostic, Indianapolis, IN, USA) was used to determine the sizes of the amplified DNA bands. The gel was stained with ethidium bromide and was visualized with UV illumination.

2.4 Reagents and protocol for RNA LAMP

Lacking the necessary safety equipment to work with viruses, we carried out the RT-LAMP experiments with the Loopamp RNA amplification kit (Eiken, Japan). The primers' composition and the amount of target analyte are considered proprietary information and are unavailable. The target analyte concentration is reported to be in the concentration range typical of clinical samples. Each RT-LAMP reaction was carried out with a 20 μL reaction volume containing 0.2 μM each of the outer primers F3 and B3, 0.8 μM each of loop primers F and B, 1.6 μM each of the primers FIP and BIP, 1.4 mM dNTPs, 0.8 M betaine, 0.1% Tween 20, 10 mM $(NH_4)_2SO_4$, 8 mM $MgSO_4$, 10 mM KCl, 20 mM Tris–HCl (pH 8.8), 8 U of Bst DNA polymerase, 0.625 units of AMV reverse transcriptase, 4.0 μM SYTO® 9 Green, and 2 μL of RNA template. The reverse transcription and amplification were carried out in a single step at 63°C. In a separate effort, Liu et al. (2011) amplified HIV RNA using our cassettes (without the thermally expandable valves) and the RT-LAMP process.

3 The integrated, real-time LAMP system

Figure 3 is a photograph of the experimental setup of the integrated LAMP cassette with the real-time fluorescence detection. The fluorescence excitation and detection were carried out with a portable optical detection system (Fluo Sens SD 003, Qiagen Lake Constance GmbH, Germany). The ESE optical detector (also shown in the inset in Fig. 3) uses 470 nm LED as the excitation light source and low-noise Si-photodiode for fluorescence detection.

In the experiment, the LAMP mixture was introduced into the LAMP cassette through the inlet port and the inlet, thermo-responsive, PDMS valve. The liquid filled the LAMP chamber, displacing the air through the outlet port. Once the liquid arrived at the outlet valve's location, both the inlet and exit, thermo-responsive PDMS valves were heated to 80°C with a flexible, polyimide-based thin film heater (Model HK5572R7.5L23A, Minco Products, Inc., Minneapolis, MN) located beneath the cassette next to the

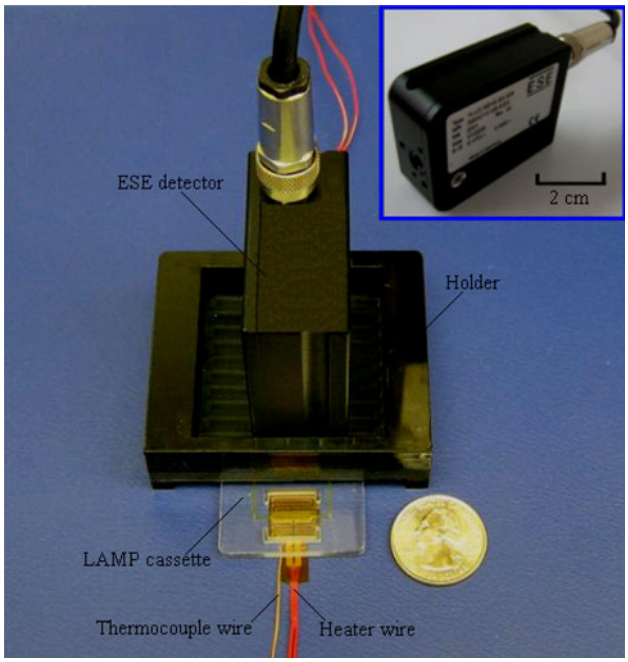

Fig. 3 LAMP-based system with real-time detection. The system consists of a single use, disposable LAMP cassette, a portable ESE detector (see also *inset*), and two thin film heaters

valves' positions (Fig. 4). Although in our experiments, the heater was powered with a DC power supply (Model 1611, B&K Precision Corporation, CA), it could be powered with a battery. When the thermo-responsive PDMS disks were heated to over 80°C, they expanded and closed the valves. Although the heaters can be readily patterned on the cassette, it is anticipated that, for economic reasons, it would be preferred to have the heaters part of a reusable reader/analyzer rather than part of the disposable cassette.

Once both the upstream and downstream valves were closed, the LAMP chamber's temperature was raised to 63°C for 1 h. The heat was supplied with a thin film heater, similar to the one used to actuate the valves, positioned beneath the LAMP chamber (Fig. 4). In the experiments reported here, the chamber's temperature was controlled in an open loop mode. To calibrate the device, we constructed a mock cassette, filled the LAMP chamber with water, and inserted into the chamber a type-K thermocouple (Omega Engr., Stamford, CT, USA). Each wire was 75 μm in diameter and the junction diameter was ~170 μm. The thermocouple reading was monitored with a HH506RA multilogger thermometer (Omega Engr., Stamford, CT, USA).

The intensity of the fluorescence signal emitted by the LAMP chamber was measured with the portable ESE optical detector. The detector was interfaced with a computer through a USB interface, and the graph of the fluorescence intensity as a function of time was displayed on the computer screen. In addition, images of the

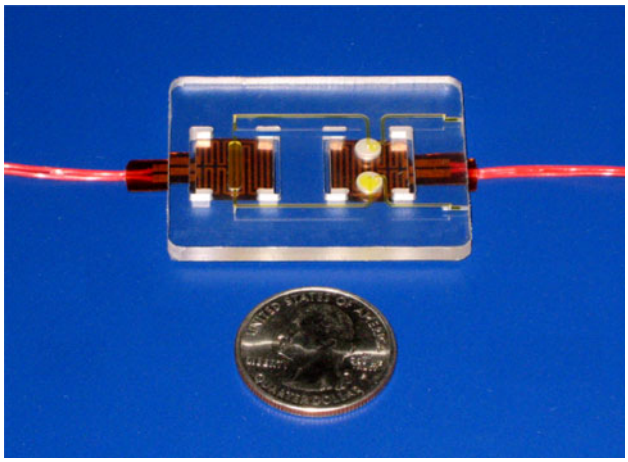

Fig. 4 A photograph of the LAMP cassette with the two thin film heaters. The left and right heaters actuate, respectively, the LAMP reaction chamber and the two valves

fluorescence of the LAMP chamber before and after the amplification process were obtained with an Olympus IX-71 inverted fluorescence microscope (Olympus America Inc., Melville, NY).

4 Results and discussion

4.1 Characterization of the thin film heating system

Figure 5 depicts the steady-state reactor's temperature as a function of the heater's power input. In the temperature range between 23°C and 95°C, the temperature depended nearly linearly on the heater's power input. In the laboratory (room temperature of ~23°C), when power of 0.32 W (1.75 V) was applied to the heater, the reactor's temperature was maintained at 63°C ± 0.2°C for the entire

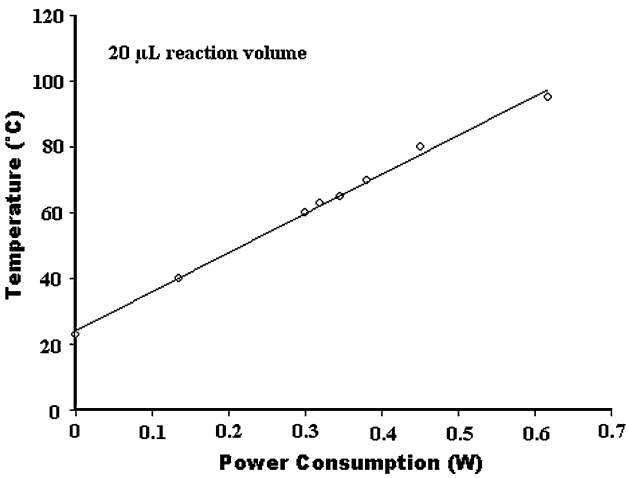

Fig. 5 The LAMP chamber's temperature as a function of the heater's power consumption

duration of the LAMP incubation process (1 h). For field operation, it would most likely be necessary to operate the heater in a closed loop control mode. The design and construction of such a control system would be relatively simple. As an interesting alternative, heat can be supplied by an exothermic chemical reaction without a need for any electrical power. For example, recently, Hatano et al. (2010) have successfully carried out LAMP amplification of *Bacillus anthracis* pag and capB gene fragments with commercially available heating packs of the type used to warm food products, albeit not in a microfluidic setting.

Although possible background fluorescence from the polyimide-based, thin film heater was of concern, we did not detect any significant emission from the heater that could interfere with our real-time LAMP detection system.

4.2 Thermo-responsive PDMS valve

The PDMS–Expancel microspheres composite is a convenient material for forming single-action, "one-shot," valves for sealing the reaction chamber. When the microspheres are heated in air to above 80°C, they expand irreversibly with about a 60-fold increase in volume. One would expect, however, a much smaller increase in the volume of the PDMS–microspheres composite.

To evaluate the expandability of the composite for various ratios of PDMS base and curing agent, we cast 4 mm diameter, 0.8 mm thick disks of thermo-responsive PDMS composite using various ratios of PDMS base, curing agent, and microspheres. Figure 6 depicts the relative change in the volume of the composite as a function of composition ($N = 3$). Not surprisingly, as the concentration of microspheres increases so does the expandability of the thermo-responsive composite. Too large a concentration of microspheres, however, increased the apparent viscosity of the PDMS blend and adversely impacted its castability and compatibility with the mold.

Samel et al. (2007a) mentioned, in passing without any details, that the ratio of the PDMS base/curing agent had no effect on expandability. We found otherwise. When the volumetric ratio of the PDMS base to the curing agent was significantly altered, the expandability varied dramatically. As the relative amount of curing agent decreased, the elasticity and the expandability of the thermo-responsive composite increased. A composite consisting of 25% microspheres by volume and a PDMS-base/curing agent ratio of 20:1 expands nearly 550% upon heating. This is a much greater expandability than the previously reported 250% for a PDMS with base/curing agent ratio of 10:1 (Samel et al. 2007a).

In addition to expandability, the compliance of the PDMS composite is a major factor that affects valve performance. As we increased the concentration of the microspheres, we

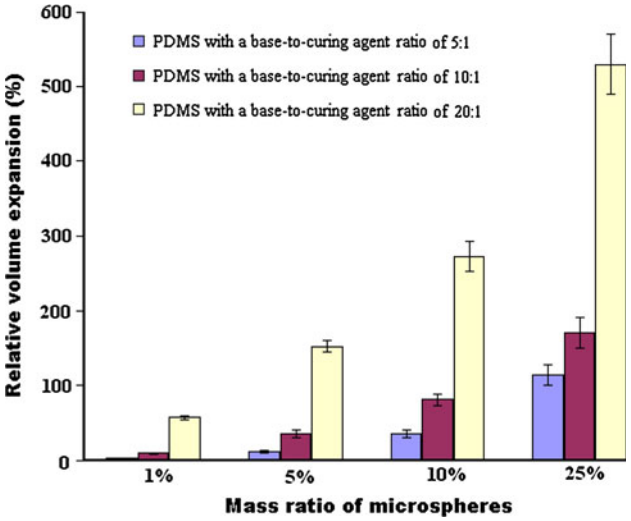

Fig. 6 The relative volume change of the thermo-responsive PDMS composite as a function of composition. The *error bars* correspond to the scatter of the data obtained in three experiments

encountered difficulties in maintaining a hermetic seal. Thus, as a trade-off between expandability and compliance, we elected to make our valves with a 5% (by volume) concentration of microspheres in a PDMS matrix with a ratio of 20:1 of base to curing agent. The resulting material expanded about 150% ± 5% upon heating.

Although the time response of the valve was not a critical factor in our application, we nevertheless measured the closing time of the valve. We define the valve response time as the time interval from the instant when the power supply was turned on to the instant when the valve fully expanded as observed visually. Figure 7 depicts the response time of the thermo-responsive valve consisting of a 4 mm diameter, 0.8 mm thick disk (20:1 base PDMS-curing agent ratio and 5% microsphere concentration) as a function of the power input. The time response decreased as the power input increased and attained an asymptotic value of about 23 s when the power supply exceeded 2 W. The time response is, of course, a function of the disk's size and the thermal capacitance of the substrate. Due to the relatively large size of our valve, its time response is relatively slow. The valve response time can be approximately related to the power input with an expression of the form $a\ln\left(\frac{bQ}{cQ-d}\right)$, where Q is the power supplied to the heater and a, b, c, and d are parameters that depend on the valve's dimensions and thermophysical properties.

Since PDMS has a low thermal conductivity (~0.15 W/m-K, Mark 1999), the valve is not heated uniformly. Microspheres next to the heater expand first in our thermoresponsive PDMS disk while microspheres located far from the heater expand only after a certain time delay. To examine the effect of valve thermal conductivity on the

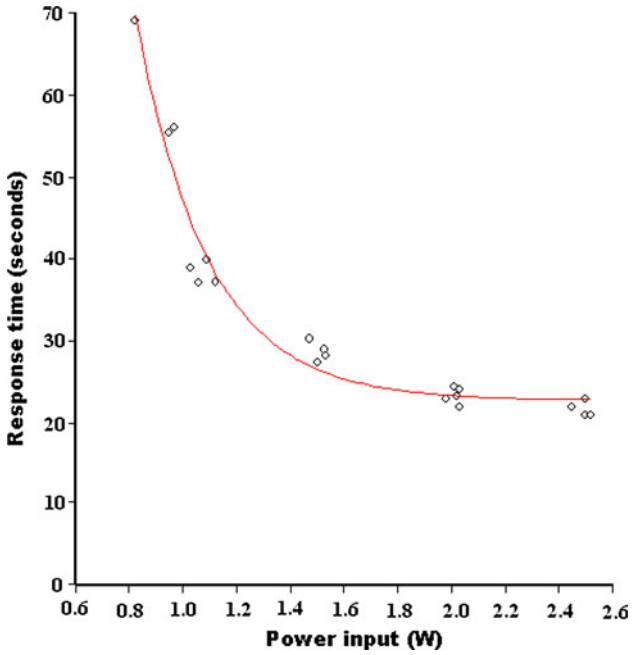

Fig. 7 The response time of the thermo-responsive PDMS valve as a function of the thin film heater's power supply

valve's performance, we varied the conductivity of the PDMS (20:1 base to curing agent ratio with 5% mass fraction of microspheres) by doping the PDMS with silver powder, and we monitored the temperatures of the valve's heated surface and the valve's distal surface as functions of time for different levels of silver doping. Figure 8 depicts

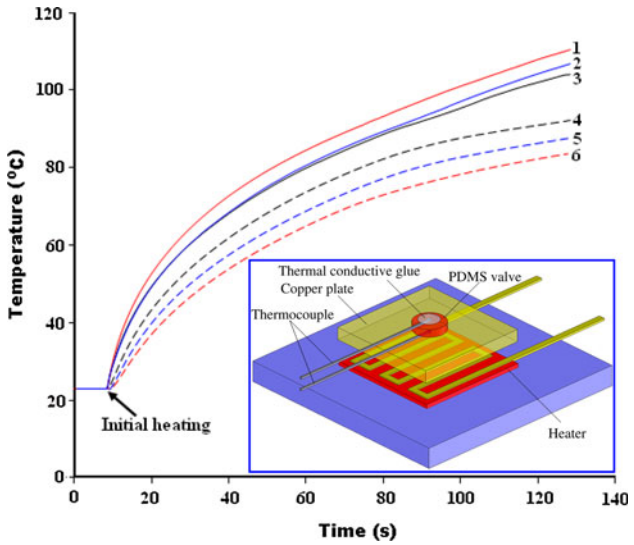

Fig. 8 The temperature of the valve's heated surface (*curves 1*, *2*, and *3*) and the valve's distal surface (*curves 4*, *5*, *6*) as functions of time in the absence of silver doping (*curves 1* and *6*), when the valve material is doped with a mass fraction of 21% silver (curves *2* and *5*) and when the valve is doped with 41% of silver by mass (*curves 3* and *4*). The power input is 0.85 W and time zero corresponds to the time when the power is turned on. The *inset* depicts the experimental set-up and the coordinates used in the theoretical model (Appendix)

the temperature of the valve's heated surface (curves 1, 2, and 3) and the valve's distal surface (curves 4, 5, 6) as functions of time in the absence of silver doping (curves 1 and 6), when the valve material is doped with a mass fraction of 21% silver (curves 2 and 5) and when the valve is doped with 41% of silver by mass (curves 3 and 4). At time $t = 0$, the heater power was set to 0.85 W. The inset depicts schematically the experimental set-up. As the silver content increases, the valve heated surface's temperature decreases, the temperature of the valve distal surface increases, and the temperature difference between the heated surface and the distal surface decreases. All are indicators that the silver doping increases the effective thermal conductivity of the PDMS composite. We estimate (see Appendix) that the increase in the effective thermal conductivity is quite modest—about a factor of 1.8 in the presence of 21% silver mass fraction and a factor of four in the presence of 41% silver mass fraction. We did not use higher doping levels out of concern for the structural integrity of the valve.

Although the silver doping increased the valve's effective thermal conductivity, it did not improve our valve's performance. Since, in our case, the gap (Fig. 2) above the valve is very small, a relatively small expansion of the PDMS suffices to achieve a good seal. Thus, it was sufficient for just a fraction of the microspheres to expand in order to close the valve. In the absence of silver doping, the temperature of the heated surface of the valve increased faster and the valve provided a faster response time. Thus, in all the experiments described from here on we used undoped valves.

The holding pressure capability of the thermo-responsive PDMS valve was measured by applying back pressure and observing leakage through the valve. The valve successfully withstood pressures as high as 200 kPa without any visible leakage, which is also suitable for sealing a PCR amplification chamber (Wang et al. 2005).

In summary, the thermo-responsive PDMS valve is easy to construct, is reliable, and exhibits reproducible performance from one device to the other. Although, given the demands of our system, we used thermo-responsive PDMS valves with dimensions in the millimeter range, the valves' size can be readily scaled down to the micrometer range with corresponding reductions in the response time and power consumption. Although not required in our application, the thermal conductivity of the valve can be controlled with appropriate doping.

4.3 Detection of DNA targets (*E. coli*)

Escherichia coli is the second major cause of neonatal meningitis, which is a major cause of mortality among newborns (Clarke 2001; Bonacorsi and Bingen 2005;

Johnson 2003; Klein et al. 2006; Marrs et al. 2005). It is also associated with a high incidence of neurological sequelae. Thus, early detection of the presence of *E. coli* is highly desirable. Here, we use the *E. coli* as a model analyte to demonstrate the ability of our cassette to detect pathogen DNA. A dilution series of *E. coli* DNA samples were isothermally amplified using the protocol detailed in Sect. 2.3, and the fluorescent intensity was monitored as a function of time.

Figure 9a and b show, respectively, the fluorescence images of the *E. coli* sample (250 target copies) in the integrated cassette before and after LAMP amplification. Figure 9a shows that the fluorescent emission from the polycarbonate and from the heater was reasonably low. Figure 9b shows significant emission resulting from the dyed, amplified product. Figure 9c depicts the real-time, fluorescence intensity as a function of time when the initial target analyte consisted of 0 (negative control), 10, 25, 100, and 250 target copies. The fluorescent intensity of the negative control (no target) remains nearly level throughout the reaction, indicating negligible formation, if any, of primer-dimers and the absence of contamination. When the target was present, the signal intensity increased from a baseline of about 1000 relative fluorescent units (RFU) to a saturated level of about 3300 RFU. The threshold time (Tt) is defined as the time that elapses from the start of the heating until the florescent signal increases $\sim$20% above the baseline level. Figure 9c indicates that Tt increases as the target molecule's concentration, C, (DNA copy number/chamber) decreases. Figure 9c (inset) depicts Tt as a function of $\log(C)$. Tt decreases nearly linearly as a function of $\log(C)$ in the range of $10 < C < 250$ copies per reaction chamber. The detection limit of 10 copies was comparable to prior reports on benchtop experiments (Hill et al. 2008). Although it is quite possible that we could have obtained a lower detection limit, we did not attempt to carry out experiments with smaller numbers of target particles since our sample dilution method could not provide us with a sufficiently accurate estimate of the number of target molecules in the reaction mix at very low target concentrations. We are aware, however, of reports on single-molecule DNA amplification and detection (Zhang and Xing 2010).

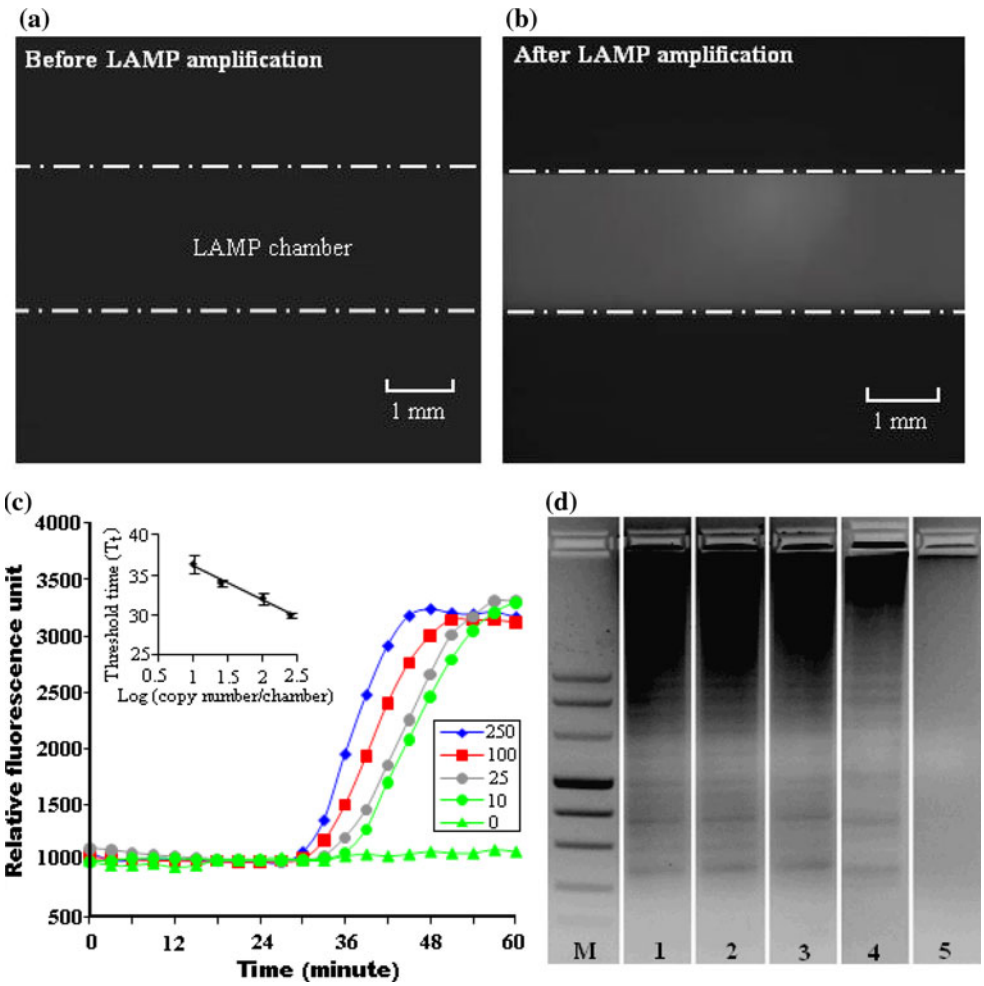

Fig. 9 Detection of *Escherichia coli* DNA in LAMP cassette: **a** image of the fluorescing LAMP chamber prior to amplification. **b** Image of the fluorescing LAMP chamber after amplification. **c** Real-time fluorescent intensity as a function of time for various concentrations of *E. coli* DNA template. *Inset*: The threshold time, Tt, (min) as a function of the DNA concentration (copies/chamber). **d** Electropherograms of LAMP products (3 μL) in a 2% agarose gel. *Lane M* is DNA marker VIII, *Lanes 1*, *2*, *3* and *4* correspond, respectively, to 250, 100, 25, 10, and 0 (negative control) copies per LAMP chamber

To verify the real-time measurements, we subjected the LAMP products to gel electrophoresis. At the conclusion of the reaction, two holes were drilled into the cassette and 3 μL of the LAMP products was removed from each chamber and subjected to electrophoretic, size-based separation. Figure 9d shows the electropherograms of ethidium bromide, stained LAMP products in 2% agarose gel. Lanes 1, 2, 3, 4, and 5 correspond, respectively, to LAMP cassette products with 250, 100, 25, 10, and 0 (negative control) copies. The gel images feature separated bands, which is a characteristic ladder structure associated with LAMP products, indicating that the DNA was successfully amplified in our cassette. In contrast to a PCR product which consists of a single length amplicon and that exhibits a single band in the electropherogram, the LAMP amplicons are connected and the product molecules have different lengths. Therefore, the electropherograms exhibit the ladder pattern. For comparison and as a control, we carried out LAMP amplifications in a bench-top PCR thermocycler (Techne Incorporated, Princeton, NJ). The benchtop experimental results, provided in Fig. 2S, show similar results to the ones obtained with the cassette.

4.4 Detection of RNA targets

Since in many instances, such as in the case of HIV infection, one is interested in detecting RNA viruses at the point of care, we explored the feasibility of carrying out single-step, reverse transcription and amplification (RT-LAMP) in our LAMP cassette. Since our laboratory is not equipped to safely handle viruses, we used the Loopamp RNA amplification kit (Eiken Chemical Co. Ltd., Japan) as the model system. Unfortunately, Eiken Chemical Co. Ltd. does not provide the sequence of primers and the concentration of RNA template. Our experiments were therefore limited to comparing the RT-LAMP products produced in the cassette with the products of a commercial benchtop device.

Figure 10a depicts the real-time RT-LAMP fluorescent intensity as a function of time for a signal resulting from a negative control (no template) and a signal generated by the Loopamp RNA kit. When target is present, the signal rises from a baseline of about 970 RFU to a saturation level of about 3300 RFU.

To verify that the LAMP cassette, indeed, produced amplicons, we extracted a fraction of the products from the cassette and carried out electrophoretic separation in gel. At the end of the reaction, two holes were drilled into the cassette and 3 μL of the LAMP products was removed from the chamber and subjected to electrophoretic, size-based separation. Figure 10b shows electropherograms of ethidium bromide-stained LAMP products in the 2% agarose gel. Lane 1 corresponds to the product of the benchtop PCR cycler (positive control). Lanes 2 and 3 correspond, respectively, to positive control (with target) and negative control (no target) RT-LAMP, cassette products. The electropherograms show the characteristic ladder structure associated with LAMP products, indicating successful amplification in our cassette. Also, note the similarity between the benchtop (lane 1) and the cassette's (lane 2) amplified products.

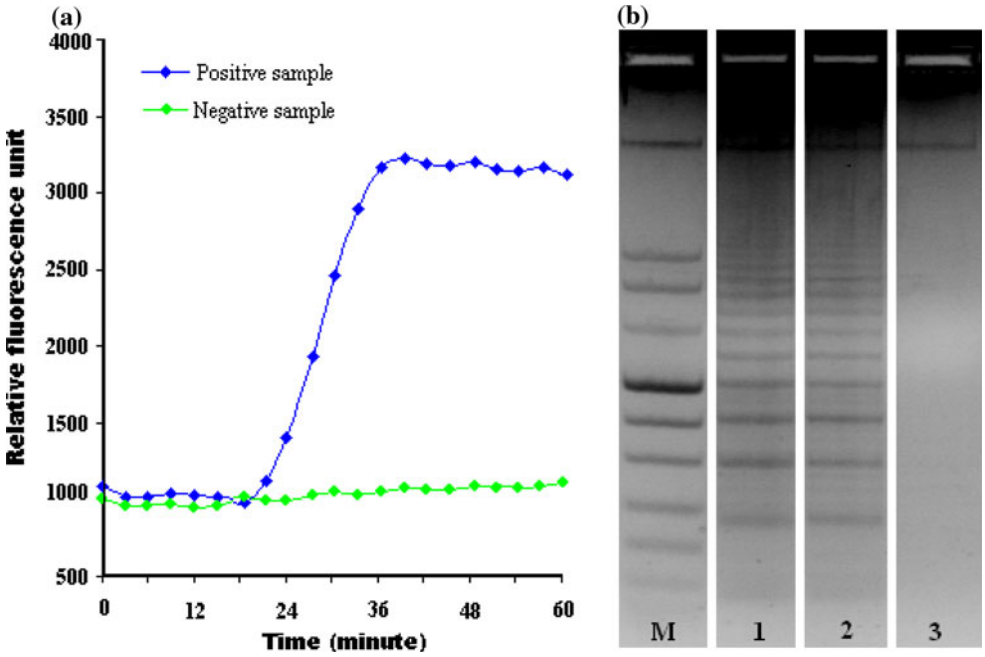

Fig. 10 RT-LAMP amplification and detection in the integrated LAMP cassette: **a** real-time fluorescence intensity as a function of time for a sample containing RNA target and a sample without any target (negative control). **b** Electropherograms RT-LAMP products (3 μL) in a 2% agarose gel. *Lane M* DNA marker VIII, *Lane 1* RT-LAMP products of benchtop PCR thermocycler; *Lanes 2* and *3* are, respectively, RT-LAMP products of positive and negative samples amplified in the integrated LAMP cassette

5 Conclusion and outlook

A new, single-use, low-cost, disposable, integrated LAMP/RT-LAMP, plastic cassette that utilizes thermo-responsive PDMS valves was developed, allowing isothermal nucleic acid amplification and on-chip, real-time monitoring of the amplification process via fluorescence detection. The device has the potential to be used as a component of a point of care device that can be operated by minimally trained personnel without any need for sophisticated laboratory equipment.

Although the idea of thermo-responsive valves, made with a PDMS–expandable microspheres mixture, was previously described in the literature (Samel et al. 2007a, b), our work demonstrates, for the first time, that the expandability of the thermo-responsive PDMS composite can be controlled by varying the volumetric ratio of the PDMS-base and curing agent and that the effective thermal conductivity of the valve material can be modified with appropriate doping. For a fixed concentration of expandable microspheres, the higher the PDMS base content, the higher the expandability. The paper also presents a new valve design that can withstand backpressures as high as 200 kPa without any observable leakage. The valves made with thermo-responsive PDMS composite are inexpensive, appropriate for disposable devices, easy to fabricate and integrate into functional microfluidic devices, robust, and reproducible. Finally, this is a first report on the integration of the expandable valve with an enzymatic amplification reactor.

Both the LAMP chamber and the valves are actuated (remotely) with thin film heaters. The heaters are part of the instrument that control the cassette and therefore do not add to the cost of the disposable cassette. The amplification results were monitored with a compact, portable ESE fluorescent detector. The use of real-time detection simplifies cassette design and eliminates the need to transfer the reaction products from the amplification reaction chamber into a separate detection chamber. The real-time detection also reduces the analysis time since the test can be stopped as soon as a detectable signal is obtained.

To demonstrate the system's utility for the detection of DNA and RNA targets, we carried out a series of experiments in which we detected *E. coli* DNA at 10 target copies and RNA positive control included in an Eiken loopamp kit. These preliminary experiments indicate that the LAMP cassette system has potential for rapid diagnosis of infectious diseases at the point of care.

Future modifications and improvements of the cassette may include dry storage of the LAMP/RT-LAMP reagents in the reaction chamber. This can be achieved by encapsulating the dry reagents with paraffin (Kim et al. 2009), which will melt upon heating the reaction chamber to the desired incubation temperature of 63°C, move out of the way, and allow the hydration of the LAMP reagents. Another improvement may include equipping the cassette with a solid state membrane for the isolation and purification of nucleic acid targets (Liu et al. 2011). It would also be desirable to operate with microspheres that expand at temperatures below 60°C so that the same heat source that is used to incubate the isothermal amplification can also be used to actuate the valves.

Acknowledgments The work was supported by NIH/NIDCR Grant U01DE017855. Professor Abhay Vats from the Children's Hospital of Pittsburgh provided useful advice and gifted template and primers for the *Escherichia coli* LAMP. Ms. Amanda Wynne Dyson machined the LAMP cassettes.

Appendix

Although not central to the manuscript, we estimated the effect of the doping on the thermal conductivity of the PDMS disk. To this end, we model the disk with a one-dimensional, steady-state model. The steady state temperature distribution along the disk's height is given by

$$T(x) - T_\infty = \frac{q}{h}\left(1 + Bi_i\left(1 - \frac{x}{H}\right)\right), \quad (1)$$

where T is the temperature at distance x above the heated surface; q is the heat flux at the heated surface; h is the heat transfer coefficient at $x = H$; H is the height of the doped PDMS disk; $Bi_i = \frac{hH}{k_i}$ is the Biot number of the doped disk; and k_i is the thermal conductivity of the doped disk. The temperature ratio $\theta_i = \frac{T(0)-T_\infty}{T(H)-T_\infty} = 1 + Bi_i$. The ratio of the thermal conductivities $\frac{k_i}{k_0} = \frac{\theta_0 - 1}{\theta_i - 1}$, where subscripts 0 and i denote, respectively, the undoped and doped disks.

References

Auroux PA, Koc Y, deMello A, Manz A, Day PJ (2004) Miniaturised nucleic acid analysis. Lab Chip 4(6):534–546

Bae B, Kim N, Kee H, Kim SH, Lee Y, Lee S, Park K (2002) Feasibility test of an electromagnetically driven valve actuator for glaucoma treatment. J Microelectromech Syst 11(4):344–354

Bonacorsi S, Bingen E (2005) Molecular epidemiology of *Escherichia coli* causing neonatal meningitis. Int J Med Microbiol 295(6–7):373–381

Chen Z, Qian S, Abrams WR, Malamud D, Bau HH (2004) Thermosiphon-based PCR reactor: experiment and modeling. Anal Chem 76(13):3707–3715

Chen Z, Wang J, Qian S, Bau HH (2005) Thermally-actuated, phase change flow control for microfluidic systems. Lab Chip 5(11): 1277–1285

Chen Z, Mauk MG, Wang J, Abrams WR, Corstjens PLAM, Niedbala RS, Malamud D, Bau HH (2007) A microfluidic system for

saliva-based detection of infectious diseases. Ann NY Acad Sci 1098:429–436
Chen G, Svec F, Knapp DR (2008) Light-actuated high pressure-resisting microvalve for on-chip flow control based on thermo-responsive nanostructured polymer. Lab Chip 8(7):1198–1204
Clarke SC (2001) Diarrhoeagenic *Escherichia coli*: an emerging problem? Diagn Microbiol Infect Dis 41(3):93–98
Compton J (1991) Nucleic acid sequence-based amplification. Nature 350(6313):91–92
Das C, Fredrickson CK, Xia Z, Fan ZH (2007) Device fabrication and integration with photodefinable microvalves for protein separation. Sens Actuators A 134(1):271–277
Dimov IK, Garcia-Cordero JL, O'Grady J, Poulsen CR, Viguier C, Kent L, Daly P, Lincoln B, Maher M, O'Kennedy R, Smith TJ, Ricco AJ, Lee LP (2008) Integrated microfluidic tmRNA purification and real-time NASBA device for molecular diagnostics. Lab Chip 8(12):2071–2078
Easley CJ, Karlinsey JM, Bienvenue JM, Legendre LA, Roper MG, Feldman SH, Hughes MA, Hewlett EL, Merkel TJ, Ferrance JP, Landers JP (2006) A fully integrated microfluidic genetic analysis system with sample-in-answer-out capability. Proc Natl Acad Sci USA 103(51):19272–19277
Fang X, Liu Y, Kong J, Jiang X (2010) Loop-mediated isothermal amplification integrated on microfluidic chips for point-of-care quantitative detection of pathogens. Anal Chem 82(7):3002–3006
Gaspar A, Piyasena ME, Daroczi L, Gomez FA (2008) Magnetically controlled valve for flow manipulation in polymer microfluidic devices. Microfluid Nanofluid 4(6):525–531
Griss P, Andersson H, Stemme G (2002) Expandable microspheres for the handling of liquids. Lab Chip 2(2):117–120
Gulliksen A, Solli LA, Drese KS, Sörensen O, Karlsen F, Rogne H, Hovig E, Sirevåg R (2005) Parallel nanoliter detection of cancer markers using polymer microchips. Lab Chip 5(4):416–420
Hatano B, Maki T, Obara T, Fukumoto H, Hagisawa K, Matsushita Y, Okutani A, Bazartseren B, Inoue S, Sata T, Katano H (2010) LAMP using a disposable pocket warmer for anthrax detection, a highly mobile and reliable method for anti-bioterrorism. Jpn J Infect Dis 63(1):36–40
Hill J, Beriwal S, Chandra I, Paul VK, Kapil A, Singh T, Wadowsky RM, Singh V, Goyal A, Jahnukainen T, Johnson JR, Tarr PI, Vats A (2008) Loop-mediated isothermal amplification assay for rapid detection of common strains of *Escherichia coli*. J Clin Microbiol 46(8):2800–2804
House DL, Chon CH, Creech CB, Skaar EP, Li D (2010) Miniature on-chip detection of unpurified methicillin-resistant *Staphylococcus aureus* (MRSA) DNA using real-time PCR. J Biotechnol 146(3):93–99
Johnson JR (2003) Microbial virulence determinants and the pathogenesis of urinary tract infection. Infect Dis Clin N Am 17(2):261–278
Kim JH, Na KH, Kang CJ, Jeon D, Kim YS (2004) A disposable thermopneumatic-actuated microvalve stacked with PDMS layers and ITO-coated glass. Microelectron Eng 73–74:864–869
Kim J, Byun D, Mauk MG, Bau HH (2009) A disposable, self-contained PCR chip. Lab Chip 9(4):606–612
Klein EJ, Boster DR, Stapp JR, Wells JG, Qin X, Clausen CR, Swerdlow DL, Braden CR, Tarr PI (2006) Diarrhea etiology in a Children's Hospital Emergency Department: a prospective cohort study. Clin Infect Dis 43(7):807–813
Lagally ET, Scherer JR, Blazej RG, Toriello NM, Diep BA, Ramchandani M, Sensabaugh GF, Riley LW, Mathies RA (2004) Integrated portable genetic analysis microsystem for pathogen/infectious disease detection. Anal Chem 76(11):3162–3170
Li HQ, Roberts DC, Steyn JL, Turner KT, Yaglioglu O, Hagood NW, Spearing SM, Schmidt MA (2004) Fabrication of a high frequency piezoelectric microvalve. Sens Actuators A 111(1):51–56
Lien K-Y, Lee S-H, Tsai T-J, Chen T-Y, Lee G-B (2009) A microfluidic-based system using reverse transcription polymerase chain reactions for rapid detection of aquaculture diseases. Microfluid Nanofluid 7(6):795–806
Liu Y, Rauch CB, Stevens RL, Lenigk R, Yang J, Rhine DB, Grodzinski P (2002) DNA amplification and hybridization assays in integrated plastic monolithic devices. Anal Chem 74(13):3063–3070
Liu RH, Bonanno J, Yang J, Lenigk R, Grodzinski P (2004) Single-use, thermally actuated paraffin valves for microfluidic applications. Sens Actuators B 98(2–3):328–336
Liu C, Qiu X, Ongagna S, Chen D, Chen Z, Abrams WR, Malamud D, Corstjens PLAM, Bau HH (2009) A timer-actuated immunoassay cassette for detecting molecular markers in oral fluids. Lab chip 9(6):768–776
Liu C, Geva E, Mauk M, Qiu X, Abrams WR, Malamud D, Curtis K, Owen M, Bau HH (2011) An isothermal amplification reactor with an integrated isolation membrane for point-of-care detection of infectious diseases. Analyst. doi:10.1039/C1AN00007A
Lutz S, Weber P, Focke M, Faltin B, Hoffmann J, Müller C, Mark D, Roth G, Munday P, Armes N, Piepenburg O, Zengerle R, von Stetten F (2010) Microfluidic lab-on-a-foil for nucleic acid analysis based on isothermal recombinase polymerase amplification (RPA). Lab Chip 10(7):887–893
Mark JE (1999) Polymer data handbook. Oxford University Press, New York
Marrs CF, Zhang L, Foxman B (2005) *Escherichia coli* mediated urinary tract infections: are there distinct uropathogenic *E. coli* (UPEC) pathotypes? FEMS Microbiol Lett 252(2):183–190
Nagamine K, Hase T, Notomi T (2002) Accelerated reaction by loop-mediated isothermal amplification using loop primers. Mol Cell Probes 16(3):223–229
Notomi T, Okayama H, Masubuchi H, Yonekawa T, Watanabe K, Amino N, Hase T (2000) Loop-mediated isothermal amplification of DNA. Nucleic Acids Res 28(12):E63
Oh KW, Ahn CH (2006) A review of microvalves. J Micromech Microeng 16(5):R13–R39
Oh KW, Rong R, Ahn CH (2005) Miniaturization of pinch-type valves and pumps for practical micro total analysis system integration. J Micromech Microeng 15(12):2449–2455
Piepenburg O, Williams CH, Stemple DL, Armes NA (2006) DNA detection using recombination proteins. PLoS Biol 4(7):e204
Ramalingam N, San TC, Kai TJ, Mak MYM, Gong HQ (2009) Microfluidic devices harboring unsealed reactors for real-time isothermal helicase-dependent amplification. Microfluid Nanofluid 7(3):325–336
Roxhed N, Rydholm S, Samel B, van der Wijngaart W, Griss P, Stemme G (2006) A compact, low-cost microliter-range liquid dispenser based on expandable microspheres. J Micromech Microeng 16(12):2740–2746
Samel B, Griss P, Stemme G (2007a) A thermally responsive PDMS composite and its microfluidic applications. J Microelectromech Syst 16(1):50–57
Samel B, Nock V, Russom A, Griss P, Stemme G (2007b) A disposable lab-on-a-chip platform with embedded fluid actuators for active nanoliter liquid handling. Biomed Microdevices 9(1):61–67
Sato K, Tachihara A, Renberg B, Mawatari K, Sato K, Tanaka Y, Jarvius J, Nilsson M, Kitamori T (2010) Microbead-based rolling circle amplification in a microchip for sensitive DNA detection. Lab Chip 10(10):1262–1266

Shao P, Rummler Z, Schomburg WK (2004) Polymer micro piezo valve with a small dead volume. J Micromech Microeng 14(2):305–309

Walker GT, Fraiser MS, Schram JL, Little MC, Nadeau JG, Malinowski DP (1992) Strand displacement amplification-an isothermal, in vitro DNA amplification technique. Nucleic Acids Res 20(7):1691–1696

Wang J, Chen Z, Mauk M, Hong KS, Li M, Yang S, Bau HH (2005) Self-actuated, thermo-responsive hydrogel valves for lab on a chip. Biomed Microdevices 7(4):313–322

Wang J, Chen Z, Corstjens PLAM, Mauk MG, Bau HH (2006) A disposable microfluidic cassette for DNA amplification and detection. Lab Chip 6(1):46–53

Yager P, Edwards T, Fu E, Helton K, Nelson K, Tam MR, Weigl BH (2006) Microfluidic diagnostic technologies for global public health. Nature 442(7101):412–418

Zhang C, Xing D (2007) Miniaturized PCR chips for nucleic acid amplification and analysis: latest advances and future trends. Nucleic Acids Res 35(13):4223–4237

Zhang C, Xing D (2010) Decreasing microfluidic evaporation loss using the HMDL method: open systems for nucleic acid amplification and analysis. Microfluid Nanofluid 9(1):17–30

Zhang C, Xu J, Ma W, Zheng W (2006) PCR microfluidic devices for DNA amplification. Biotechnol Adv 24(3):243–284